

## Aberration corrected imaging of a carbon nanotube encapsulated Lindqvist Ion and correlation with Density Functional Theory

This article has been downloaded from IOPscience. Please scroll down to see the full text article.

2012 J. Phys.: Conf. Ser. 371 012018

(<http://iopscience.iop.org/1742-6596/371/1/012018>)

View [the table of contents for this issue](#), or go to the [journal homepage](#) for more

Download details:

IP Address: 109.158.78.133

The article was downloaded on 05/07/2012 at 12:07

Please note that [terms and conditions apply](#).

# Aberration corrected imaging of a carbon nanotube encapsulated Lindqvist Ion and correlation with Density Functional Theory

J Sloan<sup>\*</sup>, E Bichoutskaia<sup>1</sup>, Z Liu<sup>2</sup>, N Kuganathan<sup>1</sup>, E Faulques<sup>1,3</sup>, K Suenaga<sup>2</sup>, I J Shannon<sup>4</sup>

Department of Physics, University of Warwick, Coventry, CV4 7AL UK.

<sup>1</sup>School of Chemistry, University of Nottingham, Nottingham, NG7 2RD UK

<sup>2</sup>Nanotube Research Center, National Institute of Advanced Industrial Science and Technology (AIST), Higashi 1-1-1, Tsukuba, 305-8565, Japan

<sup>3</sup>Institut des Matériaux Jean Rouxel, CNRS, UMR6502, Université de Nantes, 2 rue de la Houssinière, 44322 Nantes, France

<sup>4</sup>Department of Chemistry, University of Birmingham, Edgbaston, B15 2TT UK

E-mail: j.sloan@warwick.ac.uk

**Abstract.** 80 kV aberration-corrected transmission electron microscopy (AC-TEM) of discrete  $[W_6O_{19}]^{2-}$  polyoxometalate ions mounted within double walled carbon nanotubes (DWNTs) allow high precision structural studies to be performed. W atom column separations within the octahedral  $W_6$  tungsten template can be visualized with sufficient clarity that correlation with full-scale density functional theory (DFT) can be achieved. Calculations performed on the gas phase and DWNT-mounted  $[W_6O_{19}]^{2-}$  anions show good agreement, in the latter case, with measured separations between pairs of  $W_2$  atom columns imaged within equatorial  $WO_6$  octahedra and single W atoms within axial  $WO_6$  octahedra. Structural data from the tilted chiral encapsulating DWNT was also determined simultaneously with the anion structural measurements, allowing the nanotube conformation to be addressed in the DFT calculations.

## 1. Introduction

*In tandem* with the burgeoning interest in a wide diversity of nanoscale structures, associated studies into single molecules are becoming more prevalent. Advances in atomic probe-type (i.e. AFM, STM or similar) [1] and electron microscopy [2,3] atomic and molecular imaging techniques are making efficient comparison between experimentally determined discrete structures and *ab initio* or *a posteriori theory* more routine. A key aspect of these investigations is the correlation of intramolecular perturbations with effects induced by the local environment. Polyoxometalate ions (POMs) are of interest in this respect as they have an extensive structure-synthetic chemistry enabling a wide variety of ordered molecular-scale cluster anions to be produced with variable charge-ordering arrangements [4]. In the present context, they provide molecular-scale heavy atom motifs with observable symmetry than can be imaged by conventional high resolution transmission electron microscopy (HRTEM) when mounted in single or double walled carbon nanotubes (i.e. SWNTs or DWNTs) or graphene oxide [5,6]. We have previously been able to image the octahedral  $O_h$  symmetry Lindqvist  $[W_6O_{19}]^{2-}$  ion in DWNTs [5] (Fig. 1(a)) by HR-TEM and have imaged the  $W_2$ - $W_2$  atom column separations in the equatorial plane of the anion. A limitation of this study was that information from the corresponding axial W atom columns was blurred however a minimum requirement for an

effective comparison with theory is that at least two dimensions of the anion be resolvable. We demonstrate here that it is possible to do this for individual ions by aberration corrected transmission electron microscopy (AC-TEM) and also that we are able to obtain conformational information from the nanotube simultaneously [7]. This allows us to produce trial composite anions and nanotube conformations for investigating both structural and electronic interactions between the encapsulated anion and the nanotube using DFT.

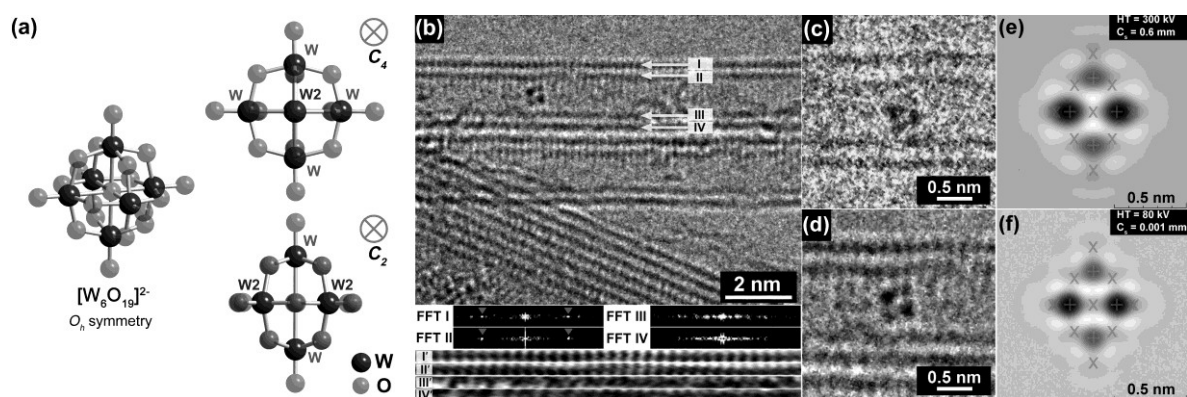


**Fig. 1** a) Perspective view,  $C_4$  projection and  $C_2$  projection of the  $[W_6O_{19}]^{2-}$  ion; b) 80 kV AC-TEM image of  $[W_6O_{19}]^{2-}$  ion in a DWNT with fast fourier transforms of the two pairs of opposing walls **I-IV** (i.e. **FFT I-FFT IV**) and corresponding filtered images (i.e. **I'-IV'**) at bottom; c) & d) Details from 300 kV ( $C_s = 0.6$  mm) image and 80 kV ( $C_s = 0.001$  mm) image of  $[W_6O_{19}]^{2-}$  ions in a DWNT. e) & f) corresponding image simulation of the  $[W_6O_{19}]^{2-}$  ion, using the same imaging conditions as c) and d).

## 2. Experimental Details

The DWNTs used in this experiment were supplied by Carbon Nanotechnology Inc.  $[nBu_4N]_2[W_6O_{19}]$  was prepared and inserted into DWNTs from an ethanolic solution. The previous 300 kV HR-TEM image of the  $[nBu_4N]_2[W_6O_{19}]@DWNT$  composite was obtained on a JEOL 3000F instrument (Oxford) with an objective  $C_s$  of 0.6 mm and a 300 kV accelerating voltage [5]. 80 kV images were obtained from the freshly prepared  $[nBu_4N]_2[W_6O_{19}]@DWNT$  composite in a JEOL 2010F AC-TEM (Tsukuba) equipped with a CEOS corrector for which  $C_s$  was tuned to 0.001 mm. Image simulations were performed using the multislice package SimulaTEM. Nanotube models were generated using the program Nanotube Modeler from JCrystalSoft (©2004-2011). Full scale CASTEP DFT calculations were performed using High Performance Computing (HPC) facility at the University of Nottingham.

## 3. Results

The previous imaging study of  $[W_6O_{19}]^{2-}$  ions mounted within DWNTs [5] revealed that within sterically matched nanotubes with an innermost  $\sim 1.2$  nm diameter SWNT the ions lie with a preferred orientation within the encapsulating cylindrical volume, specified by the van der Waals radii of the wall carbons (i.e. 0.17 nm), of diameter ca. 0.9 nm. This orientation (which is projected along the  $C_2$  rotation axis of the anion – see Fig. 1(a)) conveniently enables  $W_2$ - $W_2$  atom column pairs within the equatorial plane of the  $[W_6O_{19}]^{2-}$  superoctahedron, to be directly visualised by a conventional HR-TEM with an objective lens coefficient of spherical aberration,  $C_s$  (alternatively,  $C_s$ ), of 0.6 mm. Multislice image simulation studies showed that this level of aberration blurs the image contrast from the  $W_2$ - $W_2$  atom column pairs once the contribution of the equatorial terminal oxygen atoms is taken into account. Additionally, image contrast from the single atom W-W pair was blurred or missing. Fig. 1(b) shows a wider field of view image of two parallel DWNTs, one empty, one containing a discrete  $[W_6O_{19}]^{2-}$  anion. Comparison of a detail of the same structure anion as imaged using the 300 kV HR-TEM ( $C_s = 0.6$  mm) in Fig. 1(c) with the same structure anion using the lower voltage (i.e. 80 kV) AC-TEM ( $C_s = 0.001$  mm) imaging conditions in Fig. 1(d) shows the improvement in detail.

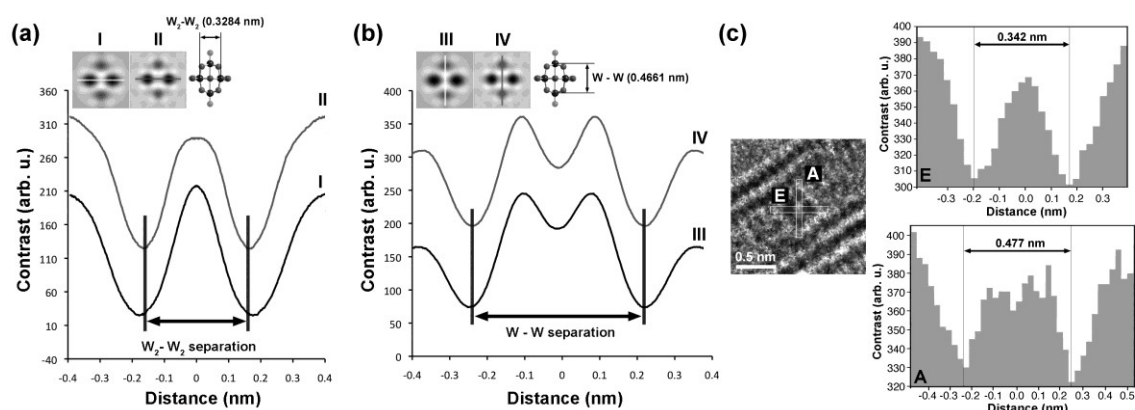


**Fig. 2** a) Line profiles through simulated equatorial  $W_2-W_2$  atom column pairs (**I** 300 kV,  $C_s = 0.6$  mm; **II** 80 kV,  $C_s = 0.001$  mm); b) as for a) but for line profiles through W-W atom column pair (**I** 300 kV,  $C_s = 0.6$  mm; **II** 80 kV,  $C_s = 0.001$  mm). c) (left) 80 kV image ( $C_s = 0.001$  mm) of the  $[W_6O_{19}]^{2-}$  ion from Figs. 1(b) and (d). (right) Experimental line profiles **E** and **A** through  $W_2-W_2$  atom column pair and W-W atom column pair respectively.

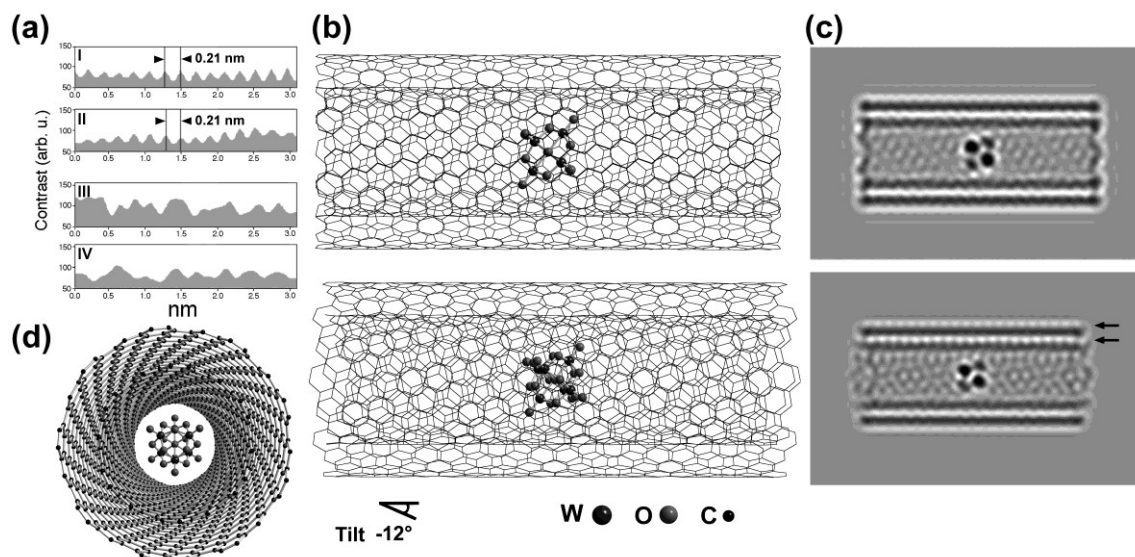


**Fig. 3** a) Line profiles **I-IV** obtained through the four filtered images **I'-IV'** in the bottom part of Fig. 1(b). The upper two walls have a periodicity of ca. 0.21 nm whereas the lower walls are aperiodic. b) Models corresponding to a  $[W_6O_{19}]^{2-}@(12,6)@(18,9)$  DWNT. The top model is untilted and the bottom model tilted  $12^\circ$  out of plane. c) Multislice image simulations from the two configurations in Fig. 4(b). Only the bottom simulation exhibits wall carbon spacings on the uppermost two walls. d) Perspective end-on model of the  $[W_6O_{19}]^{2-}@(12,6)@(18,9)$  DWNT in Fig. 2(b).

An indication of the improvement in information in the AC-TEM images can be made using line profiles through  $W_2-W_2$  and W-W atom column pairs in multislice image simulations for both cases (i.e. Figs. 1(e) and (f)) as shown by the extracted equatorial and axial profiles (i.e. Figs. 2(a) and (b)). As noted previously, there is a  $\sim 5\%$  distortion in the  $W_2-W_2$  column separation for the more aberrated case partly due to higher  $C_s$  but also to the smearing contribution of the  $O_3$  columns on the anion periphery [5]. This distortion is reproduced in Fig. 2(a) in which the troughs of profile **I** corresponding to the  $W_2$  columns are displaced  $\sim 5\%$  with respect their expected positions. Profile **II** in Fig. 2(a) corresponds to the simulated  $W_2-W_2$  atom column pairs for the AC-TEM but with  $C_s = 0.001$  mm. In this case, the troughs are displaced  $\sim 1\%$ , reflecting a greater confidence in the new measurements. According to profiles **III** and **IV** in Fig. 2(b), there is little distortion of the axial W-W columns in

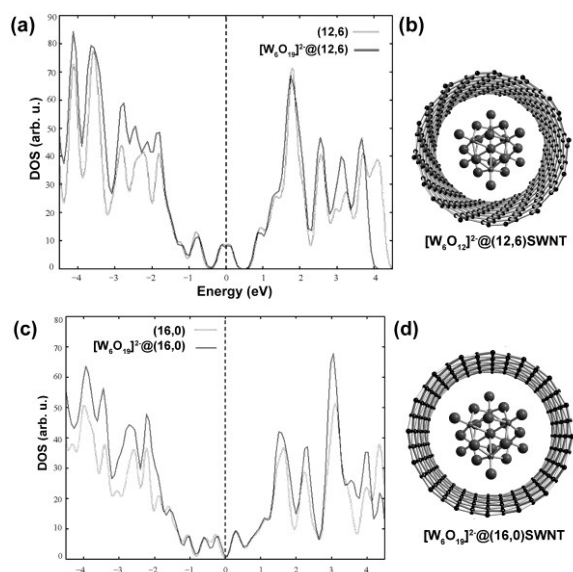


**Fig. 4** a) DOS plots for metallic  $[W_6O_{19}]^{2-}@ (12,6)$  composite. b) Optimised structure of  $[W_6O_{19}]^{2-}@ (12,6)$ SWNT. c) and d) DOS plot and optimized structure for semiconducting  $[W_6O_{19}]^{2-}@ (16,0)$ SWNT.

either the 300 kV or 80 kV images but the image contrast from the 300 kV image (Fig. 1(c)) is too noisy to produce a reliable measurement. In Fig. 2(c) we see that it is possible to measure the atom column spacings for both equatorial  $W_2$ - $W_2$  and axial  $W$ - $W$  separations for the 80 kV case (i.e. 0.342 and 0.477 nm respectively, precision  $\pm 0.026$  nm). Additionally we have also been able to resolve the wall carbon spacings on one side of the DWNT (Figs. 1(b) and (d)). Line profiles through all four walls (Fig. 3(a)) show that the top walls have an average periodicity of 0.21 nm whereas the bottom walls are aperiodic. Observation of wall carbon spacings on one side the DWNT indicates that it is chiral and tilted (Figs. 3(b) and (c)).

Reliable comparisons can now be made between the observed measurements and optimised structure models of  $[W_6O_{19}]^{2-}@$ DWNT composites produced by DFT (in practice the innermost SWNT is only considered). In the first instance, we can differentiate optimised models produced for metallic  $[W_6O_{19}]^{2-}@ (12,6)$  (Fig. 4(a) and (b)) and semiconducting  $[W_6O_{19}]^{2-}@ (16,0)$  composites (Figs. 4(c) and (d)). The densities of states (DOS) plot in Fig. 4(a) is evidently more appropriate for comparison with the experimental case. We can

also now compare both experimentally determined and DFT-optimised equatorial  $W_2$ - $W_2$  and axial  $W$ - $W$  separations. The experimental measurements for the equatorial and axial separations (i.e. 0.342 and 0.477 nm, see above) compare reasonably with the corresponding DFT optimised gas phase separations (i.e. 0.333 and 0.471 nm, respectively) and optimised  $[W_6O_{19}]^{2-}@ (12,6)$  SWNT separations (i.e. 0.331 and 0.471 nm, respectively) [7].

#### 4. Conclusions

High quality structural detail can be obtained by AC-TEM at 80 kV from DWNT-encapsulated  $[W_6O_{19}]^{2-}$  ions. The obtained structural information compares favourably that obtained from DFT and the enhanced resolution also allows for conformational information from the DWNT to be included.

#### References

- [1] Eigler D M and Schweitzer E K 1990 *Nature* **344** 524.
- [2] Smith B W, Monthieux M and Luzzi D E 1998 *Nature* **396** 323.
- [3] Sato Y, Suenaga K, Okubo S, Okazaki T and Iijima S 2007 *Nano Lett.* **7** 3704.
- [4] Volkmer D, Bredenkötter B, Tellenbröcker J, Kögerler P, Kurth D G, Lehmann P, Schnablegger H, Schwahn D, Pipenbrink M and Krebs B 2002 *J. Am. Chem. Soc.* **124** 10489.
- [5] Sloan J, Matthewman G, Dyer-Smith C, Sung A-Y, Liu Z, Suenaga K, Kirkland A I and Flahaut E 2008 *ACS Nano* **2** 966.
- [6] Sloan J, Liu Z, Suenaga K, Wilson N R, Pandey P, Perkins L M, Rourke J P and Shannon I J 2010 *Nano Lett.* **10** 4600.
- [7] Bichoutskaia E, Liu Z, Kuganathan N, Faulques E, Suenaga K, Shannon I J and Sloan J, 2012 *Nanoscale*, in press.

#### Acknowledgements

We are indebted to the Warwick Centre for Analytical Science (EPSRC Grant EP/F034210/1). E. B. acknowledges a Career Acceleration Fellowship, NanoTP ‘‘Cost’’ action and HPC. Z. L. and K. S. acknowledge support from JST-CREST and Grant-in-aid from MEXT (19054017).